ORIGINAL ARTICLE

Perpendicular orientation between dispersed rubber and polypropylene molecules in an oriented sheet

Panitha Phulkerd[1] · Yoshiaki Funahashi[1] · Asae Ito[1] · Shohei Iwasaki[2] · Masayuki Yamaguchi[1]

Abstract

An immiscible blend of isotactic polypropylene (PP) and ethylene-butene-1 copolymer (EB) (PP/EB = 70/30) containing a small amount of N,N'-dicyclohexyl-2,6-naphthalene dicarboxamide as a nucleating agent for β-form crystals was prepared by T-die extrusion. We successfully prepared an extruded sheet in which the orientation of the PP molecules is perpendicular to the deformation of the EB particles, i.e., the β-form crystals of PP are predominantly oriented perpendicular to the flow direction of the sheet plane (the transverse direction, TD), whereas the EB droplets are strongly deformed in the flow direction. It should be noted that EB barely affects the crystalline form and orientation of PP. This extraordinary structure provides unique mechanical anisotropy. The tear strength of the TD sample is significantly enhanced by the anomalous crack propagation in the machine direction (MD). Moreover, the anisotropy in tensile properties, such as the Young's modulus, yield stress, strain at break, and dynamic tensile modulus, is reduced.

Introduction

Isotactic polypropylene (PP) is widely used in various applications because it is inexpensive and lightweight. In particular, the trend in the automobile industry to use PP will continue because weight reduction is an inevitable future priority. Generally, both rigidity and high impact strength are required for material design with PP [1]. Therefore, technology using blends with rubber [1–17] and fillers [18, 19] and the addition of a nucleating agent [20–25] have been intensively studied. Various types of elastomeric materials have been employed as impact modifiers. In particular, since the development of metallocene catalysts, ethylene-butene-1, ethylene-hexene-1, and ethylene-octene-1 copolymers have been preferred for this purpose because they have low interfacial tension with PP compared with traditional ethylene-propylene copolymers. Such miscibility and/or compatibility have been predicted by the difference in statistical segment length [1, 12, 17] and packing length [8, 14, 17] and have been summarized from the perspective of the species and content of the α-olefin [2, 3, 7, 15]. The rheological properties [4, 5, 9], crystallization behavior [6, 16], and processability [10, 11] of PP blends with ethylene-α-olefin copolymers have also been elucidated. Accordingly, controlling the particle size of a rubber dispersion in a continuous PP phase improves the mechanical properties of the material. In general, low interfacial tension and viscosity matching between components enable the formation of small particles with uniform dispersion by melt blending. Furthermore, the nucleation process of PP plays a key role in the processing operation because its mechanical properties are largely dependent on the form and degree of crystallinity. It is well known that PP has various crystalline forms, such as monoclinic α-modification, trigonal β-modification, orthorhombic γ-modification, and smectic forms, which are determined by the crystallization conditions and additives [2, 3, 7, 8, 12, 14, 17]. Among all the crystalline structures, recent attention has focused on β-form crystals owing to the development of highly efficient nucleating agents such as 1,3,5-benzene-trisamide [26] and N,N'-dicyclohexyl-2,6-naphthalene dicarboxamide [27, 28]. Moreover, a recent report on the enhancement of the melting point using β-form crystals [29] should be encouraging for industrial applications.

✉ Panitha Phulkerd
panitha@jaist.ac.jp

1 School of Materials Science, Japan Advanced Institute of Science and Technology, 1-1 Asahidai, Nomi, Ishikawa 923-1292, Japan

2 New Japan Chemical Co., Ltd., 13 Yoshijima, Yaguracho, Fushimi, Kyoto 612-8224, Japan

N,N'-Dicyclohexyl-2,6-naphthalene dicarboxamide has been used to ensure the molecular orientation of the PP chains in the transverse direction (TD) [30–35]. Under suitable processing conditions, the nucleating agent appears as needle-shaped crystals in PP and is aligned with the direction of flow by hydrodynamic forces. Owing to the unique crystallization behavior of PP, in which the c-axis of the PP crystals grows perpendicular to the long axis of the needle-shaped nucleating agent by epitaxial crystallization, the PP chains orient perpendicular to the flow direction during T-die extrusion [31]. The resulting product has unique mechanical properties. Orientation control using nucleating agents is applicable to injection-molding. The peculiar orientation of the PP chains, i.e., in a plywood-like structure, prohibits crack propagation and reduces anisotropy in modulus and in thermal expansion [32, 35]. A combined approach involving the addition of rubber and the control of orientation using a specific β nucleating agent is expected to maximize the mechanical performance of PP. Although several papers have been published regarding polymer blends of PP and ethylene-α-olefin copolymers, there have been few reports describing PP blends containing a β-nucleating agent in detail [36–39]. Furthermore, in industrial applications, the molecular orientation of the PP and the rubber dispersion are controlled independently.

The present research focuses on an extruded sheet comprising PP and ethylene-butene-1 copolymer (EB) with the nucleating agent N,N'-dicyclohexyl-2,6-naphthalene dicarboxamide. The orientation of the PP molecular chains and the deformation direction of the rubber particles are investigated in detail with an evaluation of the mechanical properties.

Materials and methods

Materials

The raw materials used in the present study were a commercially available isotactic polypropylene (PP) homopolymer (SunAllomer, PM600A, melt flow rate (MFR) of 7.5 g/10 min at 230 °C, Mn 63,000, Mw 360,000) and an EB (Mitsui Chemicals, TAFER DF610, MFR of 2.2 g/10 min at 230 °C, density of 860 kg/m^3, ethylene content of 54 wt.%). N,N'-Dicyclohexyl-2,6-naphthalene dicarboxamide (New Japan Chemical, NJ Star NU-100) was used as a β-nucleating agent without further purification.

Sample preparation

Melt-mixing of PP with 0.1 wt.% of the β-nucleating agent was performed by a counter-rotating twin-screw extruder (Technovel, KZW15TW-45MG-NH) with 0.05 wt.%

3-(3,5-di-tert-butyl-4-hydroxyphenyl)propionate (Ciba, Irganox 1010) and 0.1 wt.% tris(2,4-di-tert-butyl-phenyl) phosphate (Ciba, Irgafos 168) as thermal stabilizers and 0.05 wt.% calcium stearate (Nitto Kasei Kogyo) as a neutralizing agent. The screw diameter of the extruder was 15 mm, and the length-to-diameter ratio was 45. The machine was operated at a screw rotation speed of 250 rpm. The mixing was performed at 260 °C to completely dissolve the nucleating agent in molten PP. The extruded strands were dipped in a water bath and cut into pellets approximately 2.3 mm in diameter.

The pellets of PP containing the nucleating agent and EB were fed into a single-screw extruder (Technovel, SZW25GT-28VG-STD) equipped with a T-die (300 mm wide with a 0.5 mm die lip) at a blend ratio of 70/30 (PP/EB) by weight. The output rate was 3 kg/h. The screw diameter and the length-to-diameter ratio were 25 mm and 28, respectively. The speed of screw rotation was 40 rpm. The sheet was stretched in the air gap (10 mm) between the die lip and the chill roll. The temperatures of the die and chill roll were maintained at 200 °C and 103 °C, respectively. The diameter of the chill roll was 250 mm, and the rotational speed was 1 rpm. Reference samples comprising extruded sheets of PP containing the nucleating agent and PP/EB without the nucleating agent were also prepared under conditions identical to those described above.
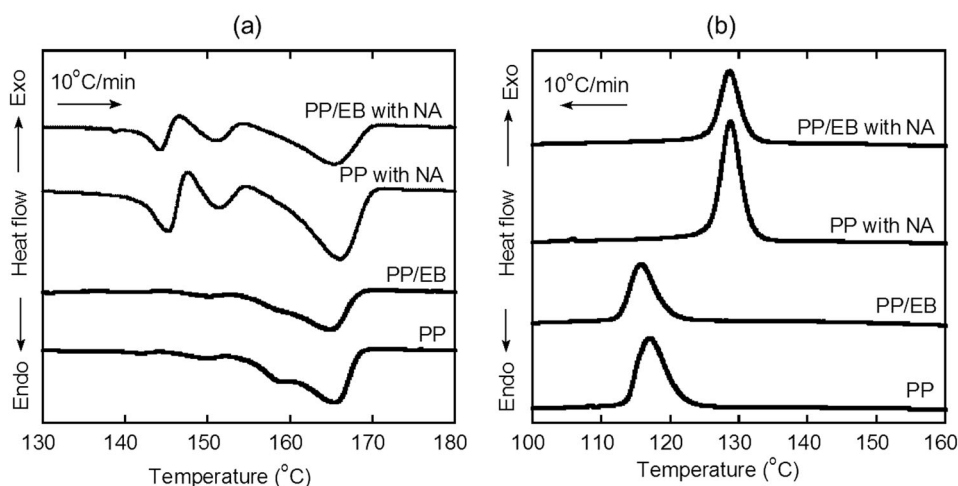
Measurements

Thermal analysis was conducted using differential scanning calorimetry (DSC) (Perkin Elmer, DSC 8000) under a nitrogen atmosphere to avoid thermal-oxidative degradation. Samples weighing approximately 3 mg were sealed in aluminium pans. The melting and crystallization profiles were recorded at a heating rate of 10 °C/min and a cooling rate of 10 °C/min.

The temperature dependence of the dynamic tensile moduli of the extruded sheets was measured between −80 °C and 175 °C using a dynamic mechanical analyzer (UBM, Rheogel-E4000-DVE). The frequency was 10 Hz, and the heating rate was 2 °C/min. The extruded sheet was cut into small rectangular pieces, 5 mm wide and 20 mm long, that were mounted between gauges at a distance of 10 mm. The measurements were carried out on two types of samples to investigate the mechanical anisotropy: one was cut parallel to the flow direction (the machine direction (MD) sample), and the other was perpendicular to the flow direction (the TD sample). In the case of the MD sample, the direction of the applied oscillatory strain coincided with the flow direction.

To analyze the crystal form of the PP molecules, X-ray diffraction (XRD) measurements were carried out in reflection mode at room temperature using an X-ray

Fig. 1 DSC profiles of the extruded sheets, **a** heating curves and **b** cooling curves

diffractometer (Rigaku, SmartLab). The measurements were carried out using CuKα radiation operated at 40 kV and 30 mA with a scanning range of 2θ (Bragg angle) from 10° to 30°. Further, the wide-angle X-ray diffraction (WAXD) patterns were collected using a high-speed two-dimensional X-ray detector (Rigaku, PILATUS 3 R 100 K) to evaluate the orientation direction of the PP molecules. Small pieces of the sample (approximately 1.0 mm thick) were mounted on the diffractometer. The X-ray beam was irradiated normal to the MD-ND plane (edge view: EV) and the MD-TD plane (through view: TV). For the EV measurements, ten sheets of the sample were laminated with polystyrene solution, whereas only one sheet was used for the TV measurements.

The orientation of the PP lamellae was investigated using transmission electron microscopy (TEM) (JEOL, JEM-2100FX) at an acceleration voltage of 200 kV. The samples were embedded in epoxy resin and sectioned using an ultramicrotome (RMC Boeckeler, Ultramicrotome MT-XL) equipped with a diamond knife after exposure to ruthenium tetroxide vapor at 40 °C for a day. Cross-sectional specimens (100 nm thick) were cut from the stained sample in the MD-ND plane.

The deformation of the dispersed EB phase was observed by scanning electron microscopy (SEM) (Hitachi, S4100) with an acceleration voltage of 20 kV. For non-conductive samples, the specimens were coated with Pt/Pd alloy for 60 s by an ion sputtering machine (Hitachi, E1010). The surfaces of the specimens were removed using a rotary microtome (Yamato Kohki Industrial, RX-860) and immersed in xylene at room temperature for 3 days to elute the rubber particles.

Stress–strain curves were generated at room temperature using a tensile machine (Tokyo Testing Machine, LSC-05/300) following ASTM D638. The specimens were cut into dumbbell-shaped pieces (10 mm wide and 40 mm long) using the No. 3 dumbbell cutter referenced in JIS K6251, reducing the sample size by 40%. The initial distance between the gauges was 30 mm, and one of the crossheads was moved up at a constant speed of 10 mm/min. Stretching was performed in two directions: one parallel to the flow direction (the MD sample) and one perpendicular to the flow direction (the TD sample). All measurements were performed at least five times, and the average values were calculated. The elongation at break was evaluated by measuring the final gauge length of the narrow part of the dumbbell.

A tear test was carried out by the Trouser method using a tensile machine (Tokyo Testing Machine, LSC-05/300). Two types of sample were cut from the extruded sheet: one had a notch parallel to the flow direction, that is, in the MD, and the other had a vertical notch, that is, in the TD). The specimens were stretched at room temperature at a speed of 200 mm/min. The distance between the gauges was 20 mm.
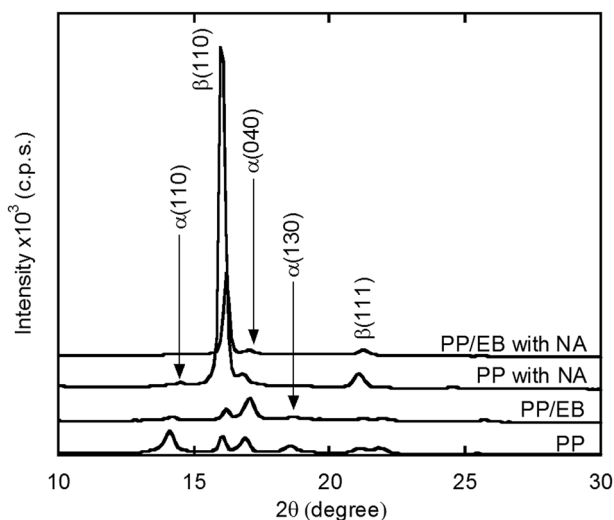
Results and discussion

Characterization of the blend sheets

The melting and crystallization behaviors of the extruded sheets are shown in Fig. 1. As shown in Fig. 1a, the pure PP sheet exhibits a main melting peak at 165 °C, suggesting α-form crystals, with a small shoulder peak of β-form crystals at 150 °C. A similar melting profile is observed for the PP/EB sheet. For the sheet containing the nucleating agent, two distinct peaks are detected at 145 °C and 151 °C, which can be attributed to β-form crystals. Furthermore, a sharp peak due to α-form crystals appears at a slightly higher temperature than that for pure PP. The recrystallization after melting of thick β-form crystals is responsible for α-form crystals with thick lamellae, leading to an enhanced melting point, as explained by Phulkerd et al. [29]. The same phenomenon is observed for the PP/EB sheet containing the nucleating agent. Under suitable

Table 1 Thermal characteristics of the extruded sheets

Sample	Crystalline form	Heat of fusion (J/g)	Crystallinity (%)
PP	α	50.9	28.8
	β	2.3	1.3
PP/EB	α	43.7	24.7
	β	2.0	1.2
PP with NA	α	59.0	33.3
	β	40.6	24.1
PP/EB with NA	α	39.1	22.1
	β	30.0	17.8

Fig. 2 XRD patterns of the extruded sheets

cooling conditions, an annealed sheet of PP containing the nucleating agent has a melting point of nearly at 170 °C due to the presence of α-form crystals [29].

The crystallization behavior during cooling from 200 °C is shown in Fig. 1b. There is no significant difference in the exothermic crystallization temperature (ca. 117 °C) between the pure PP and PP/EB sheets. After the addition of the nucleating agent, the crystallization peak shifts to a higher temperature of 128 °C for both the PP and PP/EB sheets. In this experiment, the crystallization temperature of PP is barely affected by EB, irrespective of the addition of the nucleating agent, which also indicates that EB particles hardly affect the nucleating ability of the nucleating agent.

The degrees of crystallinity of the extruded sheets are summarized in Table 1. The heats of fusion of perfect crystals of α-form and β-form PP are assumed to be 177 J/g and 168.5 J/g, respectively [40]. From the experimental results, the degrees of crystallinity of PP and PP/EB are calculated to be 30% and 26%, respectively, which correspond to mostly α-form crystals. On the other hand, the crystallinity of the β-form crystals is markedly enhanced in

the samples containing the nucleating agent. This strongly suggests that the addition of the nucleating agent enhances the crystallinity of PP.

Figure 2 shows the XRD curves of the extruded sheets. Both α- and β-form crystals are detected, but the β-form crystals are predominant in the sheets containing the nucleating agent. In the sheets without the nucleating agent, the strong peak ascribed to the α-form crystals is detected, although β(110) and β(111) peaks are still confirmed. The relatively high cooling temperature (the chill roll was maintained at 103 °C) induces β-form crystallization to a great extent. The XRD patterns also suggest that the addition of EB to PP has a negligible effect on crystal formation. Furthermore, there is an indication that the crystallinity of EB is significantly low in the extruded sheets because both the (110) and (200) planes, which are attributable to polyethylene crystals, are absent.

Figure 3 shows the 2D-WAXD patterns of the extruded sheets obtained by directing the X-ray beam in the normal direction for the edge view and in the TD for the through view. The α-form crystals in the pure PP show weak orientation, as seen in Fig. 3a. The diffraction patterns of the PP/EB sheet (Fig. 3b) are almost identical to those of the PP sheet, in which a diffraction peak attributed to the (040) plane of the α-form crystals is detected in the equatorial direction, demonstrating that the PP molecular chains are oriented in the MD. For the PP sheet containing the nucleating agent (Fig. 3c), the PP chains in the β-form crystals were oriented in the TD. Such a molecular orientation is also detected in the PP/EB sheet containing the nucleating agent, in which distinct arcs ascribed to the (110) reflection of the β-form crystals are observed, as shown in Fig. 3d. This result demonstrates that PP chains preferentially orient perpendicular to the flow direction. It also indicates that the nucleating agent promotes the growth of β-form crystals with a TD orientation of the PP molecular chains, irrespective of the presence of EB.

Figure 4 shows a TEM image of a thin slice cut along the TD-ND plane from the PP/EB sheet containing the nucleating agent. A phase-separated morphology is clearly seen in this sample, in which the dark region is the EB phase. Furthermore, the crystalline lamellae of PP are detected in the matrix as white lines, which preferentially orient along the ND. Therefore, the growth direction of the PP chains is perpendicular to the ND, i.e., in the TD orientation, which corresponds well with the XRD patterns. The compressed stress applied during the cooling process at the chill roll is responsible for the preferential TD orientation, not the ND orientation, of the PP chains. The slight deformation of EB particles toward the TD would also be attributed to the compression stress at the chill roll, although the deformation of EB particles will be explained in detail later. Furthermore, PP lamellae are incorporated into the EB phase,
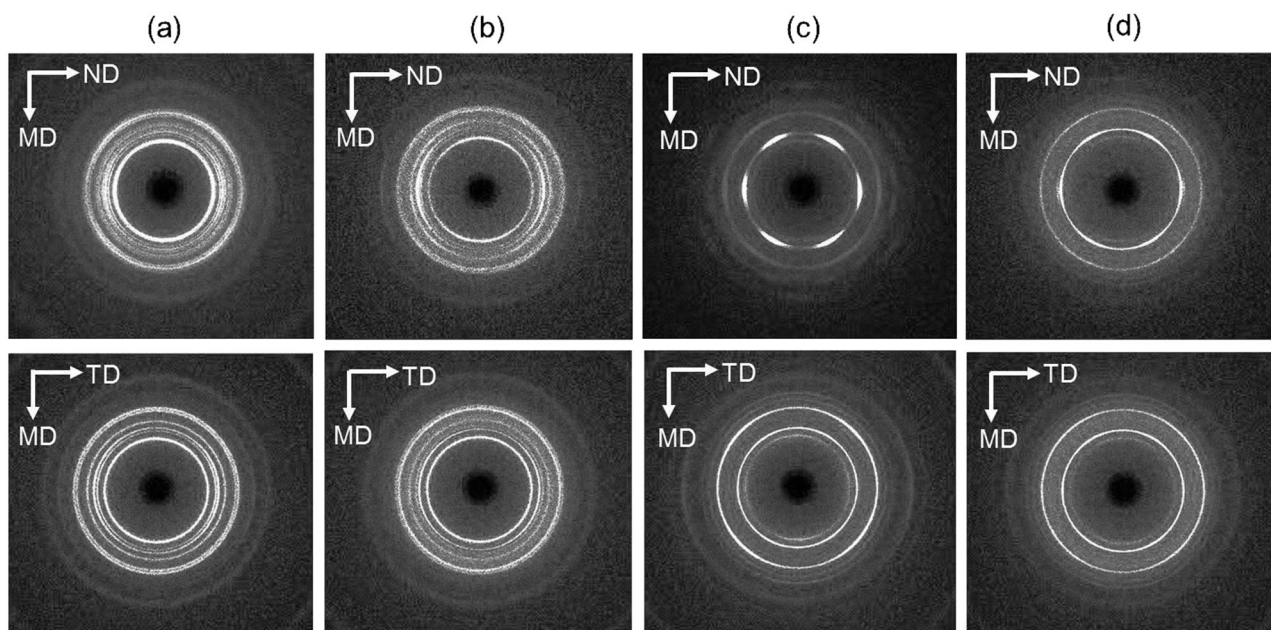
Fig. 3 WAXD patterns of the edge views (MD-ND) and through views (MD-TD) of the samples: **a** PP, **b** PP/EB, **c** PP with the nucleating agent, and **d** PP/EB with the nucleating agent. (Color figure online)

which will result in strong adhesion between them. This phenomenon is attributed to the low interfacial tension between PP and EB, leading to a large interphase thickness in the molten state.

Figure 5 shows SEM images of the PP/EB sheet containing the nucleating agent. The dark regions are attributable to the elongated pores formed by elution of the EB particles with xylene. As seen in Fig. 5a, the numerous pores are mainly deformed in the flow direction. The length of the pores is found to be approximately 3.0 µm, and the diameter is approximately 0.5 µm. On the other hand, a slight deformation in the TD with an average pore size of

Fig. 4 TEM image of the TD-ND plane (×15,000) of PP/EB with the nucleating agent

1.0 µm for the length and 0.5 µm for the diameter is detected in the TD-ND plane, owing to the pressure applied by the chill roll, which corresponds with the TEM image. The marked difference in pore size between the MD and TD demonstrates that EB preferentially orients in the flow direction. This is understandable because the elongational stress in the air gap and the shear stress in the die deform the EB particles in the flow direction via the hydrodynamic force. Similar SEM images were obtained for the PP/EB sheet without the nucleating agent (not presented here). This suggests that the nucleating agent hardly affects the rubber dispersion and deformation.
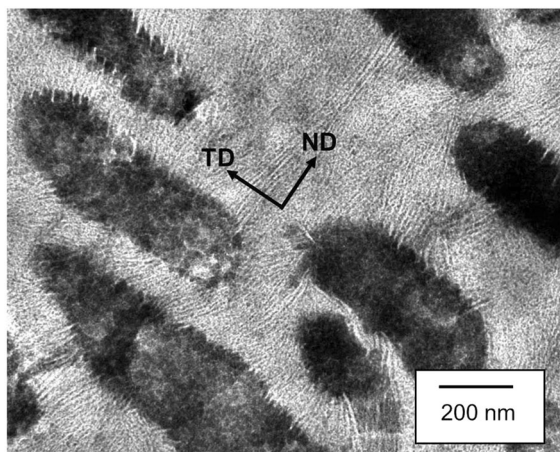
Mechanical properties

Because the molecular orientation of PP is different from that of EB, the sample sheet exhibits anomalous mechanical properties. Figure 6 shows the dynamic mechanical properties of the extruded sheets, employing two specimens to apply the oscillatory stain in different directions, i.e., the MD and TD. As seen in Fig. 6a, both the MD and TD samples of the pure PP sheet show almost the same dynamic tensile moduli over the whole range of temperatures. In contrast, for the PP sheet containing the nucleating agent (Fig. 6b), E' in the TD is higher than that in the MD at low temperatures, and vice versa at high temperatures. The crossing point of E' is detected at approximately T_g, i.e., the glass transition temperature. The anisotropy in the tie chain fraction is responsible for the crossing behavior in the sample containing the nucleating agent. The MD orientation
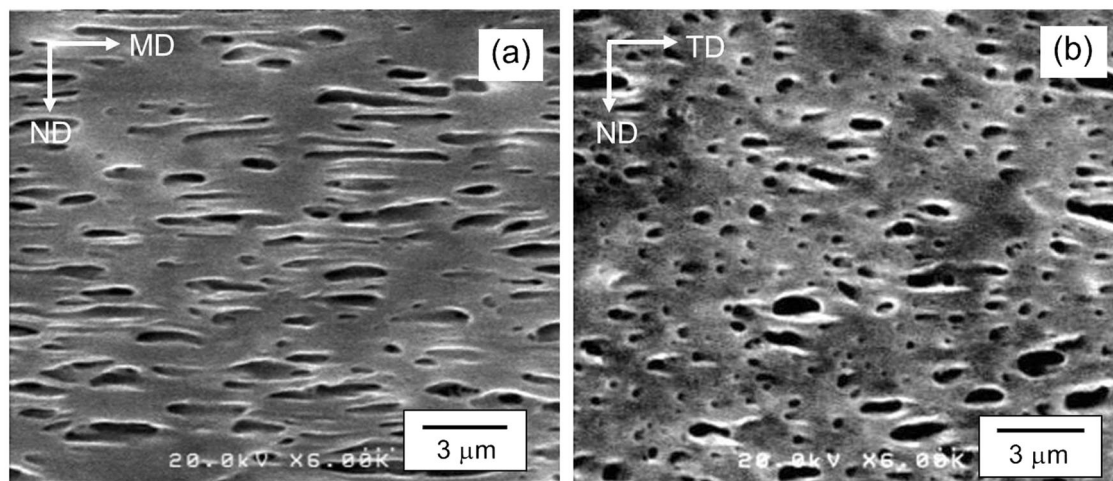
Fig. 5 SEM images of PP/EB with the nucleating agent: **a** MD-ND plane and **b** TD-ND plane

of amorphous chains was confirmed by the infrared dichroic ratio in our previous paper [33]. Because a large number of tie chains oriented in the MD by the hydrodynamic forces connecting neighboring lamellae, the higher modulus in the MD sample is reasonable. In Fig. 6c, the PP/EB sheet shows a similar behavior to that of the PP sheet, in which PP molecules orient to the flow direction. Since the molecular

orientation is weak, no obvious mechanical anisotropy is observed for the sample sheets without the nucleating agent. Moreover, E' in PP/EB falls off markedly at approximately 165 °C, which is attributed to the melting of α-form crystals. The mechanical behavior of the PP/EB sheet containing the nucleating agent (Fig. 6d) is similar to that of the PP containing the nucleating agent, but the crossing behavior of

Fig. 6 Temperature dependence of the dynamic tensile modulus of extruded sheets at 10 Hz: **a** PP, **b** PP with the nucleating agent, **c** PP/EB, and **d** PP/EB with the nucleating agent. The applied strains were parallel to the flow direction (MD) and perpendicular to the flow direction (TD)
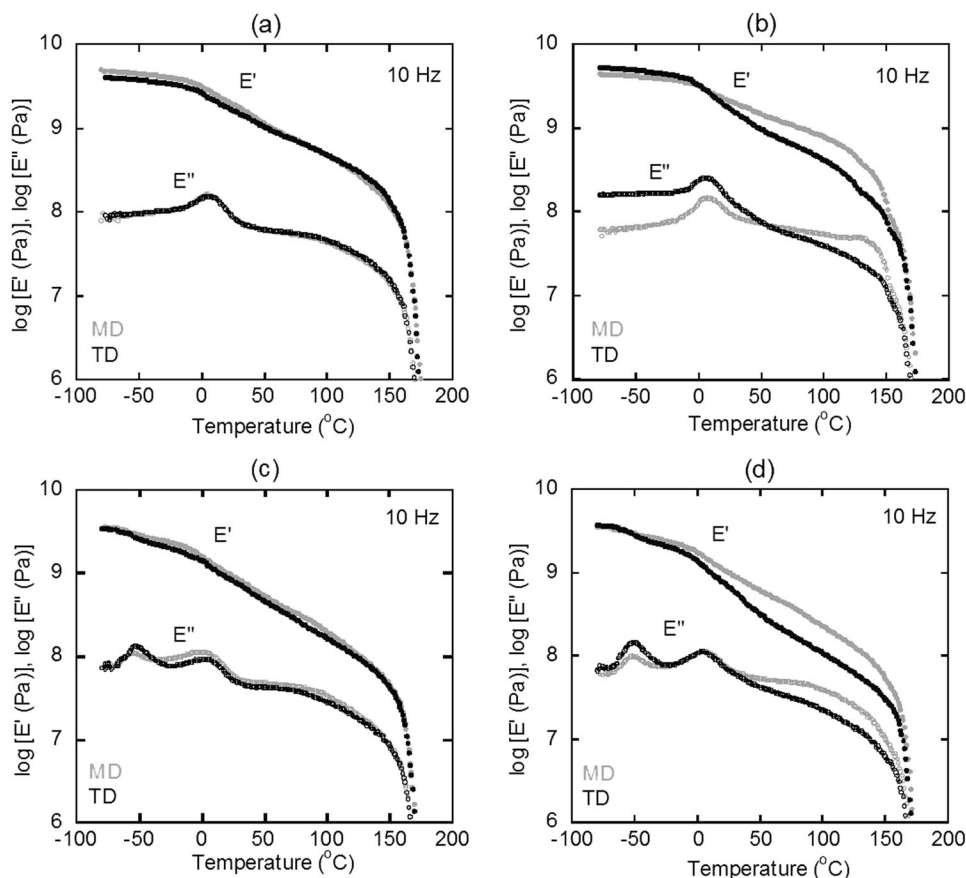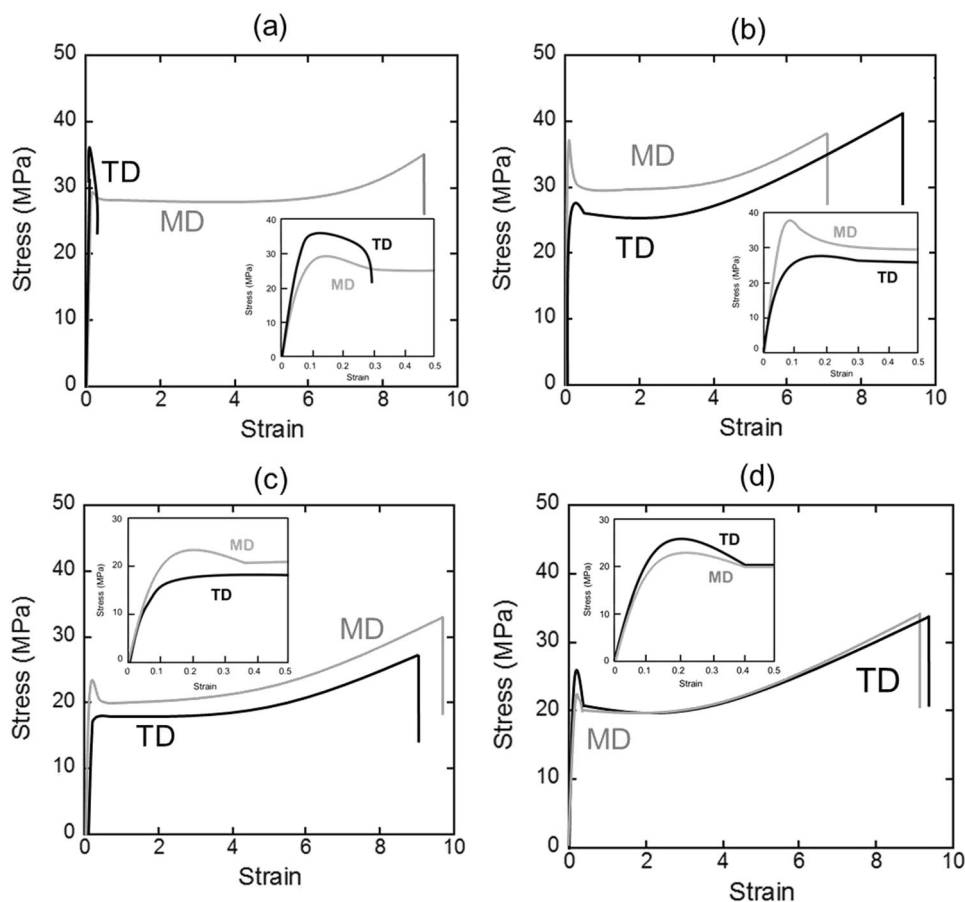
Fig. 7 Stress–strain curves of **a** PP, **b** PP with the nucleating agent, **c** PP/EB, and **d** PP/EB with the nucleating agent at a strain rate of $0.006\,\mathrm{s^{-1}}$

the former is weaker and shifted to a lower temperature region compared to that of the latter. Compared with the PP/EB sheet, the addition of the nucleating agent enhances E' for the MD sample over a wide temperature range above the glass transition temperature (T_g), owing to the high degree of crystallinity resulting from the nucleation effect. Furthermore, a sharp decrease in E' is detected at approximately 150 °C due to the melting of the β-form crystals, in agreement with the DSC and WAXD results. It is found from Fig. 6c, d that the PP/EB sheets both with and without the nucleating agent exhibit double peaks in the E'' curve in the temperature range from −75 °C to 40 °C; the peak at the higher temperature is attributed to the T_g of PP, and that at the lower temperature is attributed to the T_g of EB.
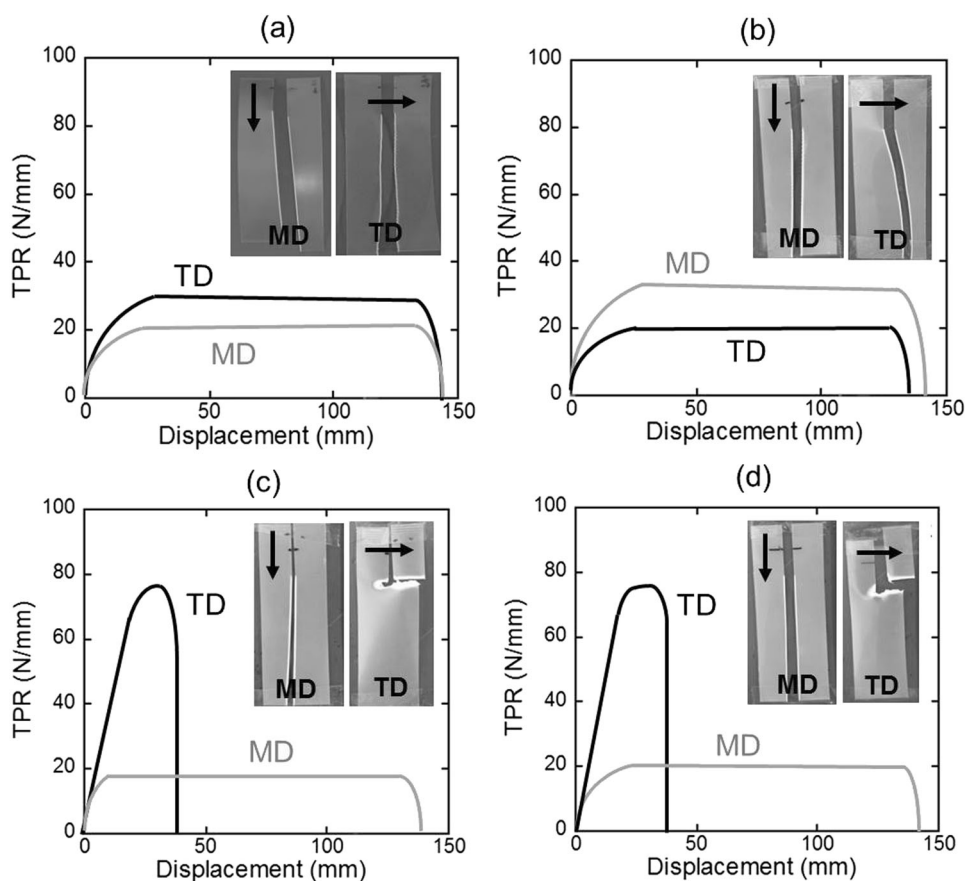
The stress–strain curves at a strain rate of $0.006\,\mathrm{s^{-1}}$ are shown in Fig. 7. The tensile force was applied along the MD or TD. The tensile properties of the extruded sheets, such as the yield stress, Young's modulus, and strain at break, are summarized in Table 2. The difference in the tensile behavior between stretching in the MD and TD is detected in all samples. As seen in Fig. 7a, the pure PP sheet experiences a brittle fracture with TD stretching beyond the yield point. In the case of MD stretching, however, ductile deformation occurs under a low yield stress. The PP

containing the nucleating agent (Fig. 7b) has a high Young's modulus due to the effect of the nucleating agent, leading to an increase in the crystallinity, which agrees with the tensile storage modulus evaluated by the dynamic mechanical measurements. Moreover, the yield stress in MD stretching is greatly enhanced in a ductile manner. The low modulus of EB is responsible for the marked decrease in Young's modulus and yield stress for both the PP/EB and PP/EB containing the nucleating agent, as seen in Fig. 7c, d. In the PP/EB sheet containing the nucleating agent, the anisotropy

Table 2 Tensile properties of the extruded sheets

Sample	Drawing direction	Yield stress (MPa)	Young's modulus (MPa)	Strain at break
PP	MD	29.6	628	9.3
	TD	35.8	701	0.5
PP with NA	MD	37.8	766	7.2
	TD	28.3	557	9.2
PP/EB	MD	23.9	415	9.7
	TD	18.6	346	9.0
PP/EB with NA	MD	22.3	311	9.3
	TD	25.4	244	9.4

Fig. 8 Tear propagation resistance (TPR) versus the applied displacement of notched specimens in the MD and TD: **a** PP, **b** PP with the nucleating agent, **c** PP/EB, and **d** PP/EB with the nucleating agent. (Color figure online)

in Young's modulus and yield stress is considerably weaker than that in the PP sheet containing the nucleating agent. The strain at break for the TD stretching of PP containing the nucleating agent is considerably larger than that of pure PP. Ductile behavior is also observed during MD stretching, although the yield stress is high. As a result, the anisotropy of the strain at break decreases following the addition of the nucleating agent. The reduction of the mechanical anisotropy is more apparent for the blend containing EB, although it is interesting to note that the PP/EB material exhibits ductile behavior not only during MD stretching but also during TD stretching. Since the yield stress of TD stretching is lower than that of MD stretching, the deformation of EB particles in the flow direction greatly affects the stress–strain behavior, although the deformation behavior of the EB phase was not revealed in this study. The details of the mechanical anisotropy in terms of crack propagation are discussed below.

A trouser tear test was carried out at room temperature employing two types of the sheet samples: one with a parallel notch in the flow direction (MD) and one with a vertical notch (TD). As seen in Fig. 8a, the pure PP sheet shows a higher tear strength in the TD sample. For PP containing the nucleating agent (Fig. 8b), the order is opposite, with enhanced anisotropy in the tear strength. In

the case of the blend, the tear strength of the TD sample is markedly enhanced, irrespective of the presence of the nucleating agent. Furthermore, the direction of crack propagation changes to the MD immediately after the stretching, as demonstrated in Fig. 8c, d. These results demonstrate that the PP orientation has no marked impact on the tear properties. The deformation of EB particles plays a dominant role in the tearing. Such information has never been reported before to the best of our knowledge because the deformation direction of a dispersion is always the same as the molecular orientation direction of the matrix, in general. Regarding the effect of the nucleating agent, the tear strength of the MD sample is slightly enhanced, although the effect is not as obvious as that in pure PP.

Conclusions

An extruded sheet with a unique structure was developed using a blend comprising PP, EB, and a small amount of N, N′-dicyclohexyl-2,6-naphthalene dicarboxamide. It was found that the nucleating agent promotes the formation of β-form crystals and causes the PP chains to orient perpendicular to the flow direction in an extruded sheet, i.e., in the TD, as confirmed by 2D-WAXD and TEM data. In contrast,

EB is deformed in the flow direction, as revealed by SEM images. As a result, the chain orientation of the PP molecules is perpendicular to the deformation direction of the EB droplets, which affects the mechanical anisotropy to a great extent. With regard to the tensile properties, the anisotropy in the yield stress and strain at break is significantly decreased owing to this peculiar structure. The tear test proved that the strength of the TD sample increases with crack growth in the flow direction. This result demonstrates that the deformation of the EB particles in the MD exhibits a more pronounced effect than the molecular orientation of the PP chains in the TD.

Compliance with ethical standards

Conflict of interest The authors declare that they have no competing financial interests.

References

1. Bates FS, Fredrickson GH. Conformational asymmetry and polymer-polymer thermodynamics. Macromolecules. 1994;27:1065–7.
2. Yamaguchi M, Miyata H, Nitta K-H. Compatibility of binary blends of polypropylene with ethylene-α-olefin copolymer. J Appl Polym Sci. 1996;62:87–97.
3. Weimann PA, Jones TD, Hillmyer MA, Bates FS, Londono JD, Melnichenko Y, Wignall GD, Almdal K. Phase behavior of isotactic polypropylene-poly(ethylene/ethylethylene) random copolymer blends. Macromolecules. 1997;30:3650–7.
4. Carriere CJ, Silvis HC. The effects of short-chain branching and comonomer type on the interfacial tension of polypropylene-polyolefin elastomer blends. J Appl Polym Sci. 1997;66:1175–81.
5. Yamaguchi M, Nitta K-H, Miyata H, Masuda T. Rheological properties for binary blends of i-PP and ethylene-1-hexene copolymer. J Appl Polym Sci. 1997;63:467–74.
6. Yamaguchi M, Miyata H, Nitta K-H. Structure and properties for binary blends of isotactic polypropylene with ethylene-α-olefin copolymer. 1. Crystallization and morphology. J Polym Sci B Polym Phys. 1997;35:953–61.
7. Thomann Y, Suhm J, Thomann R, Bar G, Maier RD, Mülhaupt R. Investigation of morphologies of one- and two-phase blends of isotactic poly(propene) with random poly(ethane-co-1-butene). Macromolecules. 1998;31:5441–9.
8. Lohse DJ, Graessley WW. Thermodynamics of polyolefin blends. In: Paul DR, Bucknall CB editors. Ch. 8. John Wiley & Sons, New York, NY, USA:John Wiley & Sons;1999. p. 219–37.
9. Yamaguchi M, Miyata H. Influence of stereoregularity of polypropylene on miscibility with ethylene-1-hexene copolymer. Macromolecules. 1999;32:5911–6.
10. Yamaguchi M, Suzuki K-I, Miyata H. Structure and mechanical properties for binary blends of polypropylene and ethylene-1-hexene copolymer. J. Polym. Sci. B Polym Phys. 1999;37:701–13.
11. Bedia EL, Murakami S, Senoo K, Kohjiya S. Structural development and mechanical properties on immiscible and miscible blends from isotactic polypropylene and ethylene-1-hexene copolymers under uniaxial drawing. Polym (Guildf). 2002;43:749–55.
12. Jones TD, Chaffin KA, Bates FS. Effect of tacticity on coil dimensions and thermodynamic properties of polypropylene. Macromolecules. 2002;35:5061–8.
13. Pasquini N. Polypropylene morphology. In: Pasquini N, editor. Ch. 3. 2nd ed. Hanser, Munich, Germany:Hanser; 2005. p. 153–94.
14. Lohse DJ. The Influence of chemical structure on polyolefin melt rheology and miscibility. J Macromol Sci Polym Rev. 2005;45:289–308.
15. Nitta KH, Yamaguchi M. Morphology and mechanical properties in iPP/polyolefin-based copolymer blend. In: Nwabunma D, Kyu T, editors. Ch. 9. New Jersey, USA: John Wiley & Sons; 2008. p. 224–68.
16. Yang J, White JL. Crystallization behavior of polypropylene/ethylene-butene copolymer blends. J Appl Polym Sci. 2012;126:2049–58.
17. Xu J, Mittal V, Bates FS. Toughened isotactic polypropylene: Phase behavior and mechanical properties of blends with strategically designed random copolymer modifiers. Macromolecules. 2016;49:6497–506.
18. Lin Y, Chen H, Chan C-M, Wu J. High impact toughness polypropylene/CaCO3 nanocomposites and the toughening mechanism. Macromolecules. 2008;41:9204–13.
19. Wiwattananukul R, Fan B, Yamaguchi M. Improvement of rigidity for rubber-toughened polypropylene via localization of carbon nanotubes. Comp Sci Technol. 2017;141:106–12.
20. Feng Y, Jin X, Hay JN. Effect of nucleating agent addition on crystallization of isotactic polypropylene. J Appl Polym Sci. 1998;69:2089–95.
21. Varga J, Mudra I, Ehrenstein GW. Highly active thermally stable β-nucleating agents for isotactic polypropylene. J Appl Polym Sci. 1999;74:2357–68.
22. Jang G-S, Cho W-J, Ha C-S. Crystallization behavior of polypropylene with or without sodium benzoate as a nucleating agent. J Polym Sci B Polym Phys. 2001;39:1001–16.
23. Marco C, Gomez MA, Ellis G, Arribas JM. Activity of a β-nucleating agent for isotactic polypropylene and its influence on polymorphic transitions. J Appl Polym Sci. 2002;86:531–9.
24. Zhu P-W, Tung J, Phillips A, Edward G. Morphological development of oriented isotactic polypropylene in the presence of a nucleating agent. Macromolecules. 2006;39:1821–31.
25. Liu M, Guo B, Du M, Chen F, Jia D. Halloysite nanotubes as a novel β-nucleating agent for isotactic polypropylene. Polym (Guildf). 2009;50:3022–30.
26. Kerscha M, Schmidtb HW, Altstädta V. Influence of different beta-nucleating agents on the morphology of isotactic polypropylene and their toughening effectiveness. Polym (Guildf). 2016;98:320–6.
27. Romankiewicz A, Sterzynski T, Brostow W. Structural characterization of α- and β-nucleated isotactic polypropylene. Polym Int. 2004;53:2086–91.
28. Zhang YF, Luo XX, Zhu L, Yang XJ, Chang Y. Effects of α/β compound nucleating agents on mechanical properties and crystallization behaviors of isotactic polypropylene. J Macromol Sci B. 2012;51:2352–60.
29. Phulkerd P, Arayachukeat S, Huang T, Inoue T, Nobukawa S, Yamaguchi M. Melting point elevation of isotactic polypropylene. J Macromol Sci B. 2014;53:1222–30.
30. Uchiyama Y, Iwasaki S, Ueoka C, Fukui T, Okamoto K, Yamaguchi M. Molecular orientation and mechanical anisotropy of polypropylene sheet containing N,N'-dicyclohexyl-2,6-naphthalenedicarboxamide. J Polym Sci B Polym Phys. 2009;47:424–33.
31. Yamaguchi M, Fukui T, Okamoto K, Sasaki S, Uchiyama Y, Ueoka C. Anomalous molecular orientation of isotactic polypropylene sheet containing N,N'-dicyclohexyl-2,6-naphthalenedicarboxamide. Polym (Guildf). 2009;50:1497–504.

32. Yamaguchi M, Irie Y, Phulkerd P, Hagihara H, Hirayama S, Sasaki S. Plywood-like structure of injection-moulded polypropylene. Polym (Guildf). 2010;51:5983–9.

33. Phulkerd P, Nobukawa S, Uchiyama Y, Yamaguchi M. Anomalous mechanical anisotropy of β form polypropylene sheet with N,N'-dicyclohexyl-2,6-naphthalene- dicarboxamide. Polym (Guildf). 2011;52:4867–72.

34. Phulkerd P, Hagihara H, Nobukawa S, Uchiyama Y, Yamaguchi M. Plastic deformation behavior of polypropylene sheet with transversal orientation. J Polym Sci B Polym Phys. 2013;51:897–906.

35. Phulkerd P, Hirayama S, Nobukawa S, Inoue T, Yamaguchi M. Structure and mechanical anisotropy of injection-molded polypropylene with a plywood structure. Polym J. 2014;46:226–33.

36. Varga J, Mudra I, Ehrensten GW. Highly active thermally stable β-nucleating agents for isotactic polypropylene. J Appl Polym Sci. 1999;74:2357–68.

37. Grein C, Gahleitner M. On the influence of nucleation on the toughness of iPP/EPR blends with different rubber molecular architectures. Express Polym Lett. 2008;2:392–7.

38. Chen Y, Yang S, Yang H, Zhang M, Zhang Q, Li Z. Toughness reinforcement in carbon nanotube-filled high impact polypropylene copolymer with β-nucleating agent. Ind Eng Chem Res. 2016;55:8733–42.

39. Sato S, Maeda T, Yamaguchi M. Control of chain orientation in blends of polypropylene and polybutene-1. Macromol Mater Eng. 2017;302:1600413–1600421.

40. Li JX, Cheung WL, Jia D. A study on the heat of fusion of β-polypropylene. Polym (Guildf). 1999;40:1219–22.